Exp Brain Res (2002) 142:268–274
DOI 10.1007/s00221-001-0932-5

RESEARCH ARTICLE

Ulrich Egert · D. Heck · A. Aertsen

Two-dimensional monitoring of spiking networks in acute brain slices

Received: 5 June 2001 / Accepted: 3 October 2001 / Published online: 10 November 2001

Abstract To understand spatiotemporally coordinated activity in neural networks and interaction between different areas or layers in brain tissue, simultaneous multisite recording is a prerequisite. For in vitro studies pursuing these goals, substrate integrated, planar microelectrode arrays (MEAs) have been developed to monitor spikes and local field potentials. Here we report for the first time recordings of single-unit spike activity with MEAs in acute slice preparations of the rat cerebellum. We compare these recordings to results of conventional techniques, and discuss the recording conditions in view of the equivalent circuits commonly used. Simultaneous recordings with tungsten microelectrodes and MEAs verified that recording characteristics and signal-to-noise ratios of MEA electrodes were comparable to those of conventional extracellular electrodes. Spike shapes were identical on both electrodes. We found no detectable overlap between spike signals recorded at neighboring MEA electrodes (200 µm spacing). Neuronal spike activity was detected with MEA electrodes at distances of up to 100 µm from the site of spike generation. We conclude that extracellular recording of independent single-unit spike activity with MEAs is indeed suitable to monitor network activity in acute slices, making MEAs an exceptionally useful tool for the assessment of fast network dynamics in acute slices.

Keywords Microelectrode arrays · Cerebellum · Brain slices · Spatiotemporal structure of spike activity · Network activity

Experimental evidence indicates that the spatiotemporal organization of neuronal activity plays a crucial role in information processing in the neocortex (Abeles et al. 1993a, 1993b; Riehle et al. 1997). To capture spatiotemporally structured spike activity, single-unit neuronal activity must be recorded at many different sites simultaneously. Furthermore, these recordings need to be mechanically and physiologically stable to allow recording times sufficiently long to yield relevant samples of spike activity, or to evaluate synaptic plasticity resulting from neuronal interaction.

Recently, substrate-integrated, planar microelectrode arrays (MEAs) have been introduced to record neuronal activity in in-vitro preparations with up to 70 electrodes simultaneously. These devices have been successful in detecting local field potentials (LFPs) and spike activity in cultures of dissociated spinal cord and cortical cell cultures (Gross et al. 1993, 1997), individual Retzius cells, acute retina preparations and cardiac myocytes (Brivanlou et al. 1998; Fejtl et al. 1998; Kamioka et al. 1996; Hämmerle et al. 1994; Meister et al. 1994; Connolly et al. 1990; Wheeler and Novak 1986). It seems likely that in these preparations neurons lie on or even grow directly on the surface of the electrodes. Similarly, acute retina preparations adhere to the electrode with a clean tissue surface and thus establish tight contact with the surface of the electrode.

In spite of this range of preparations, the recording of spike activity in the most widely used application, acute slice of brain tissue, has not yet been described in MEA recordings. In acute slices, the tissue surface of the slices is covered with a layer of dead or injured cells and cell fragments produced by the cutting process. This layer of debris prevents close contact between intact, active neurons and the recording electrode, thereby presumably reducing the seal resistance (R_s) between the signal source and the reference electrode in acute brain slice preparations. Typically, only the comparatively large electrical fields of LFPs were readily detected (Grattarola and Martinoia 1993; Wheeler and Novak 1986; Wheeler et al. 1989). The detection of the smaller extracellular fields generated by individual spikes has not been reported yet, and has commonly been assumed to be hindered by an insufficient R_s in acute slices.

U. Egert (✉) · D. Heck · A. Aertsen
Neurobiology and Biophysics, Institute of Biology III,
Albert-Ludwigs Universität Freiburg, Schänzlestr. 1,
79104 Freiburg, Germany
e-mail: egert@biologie.uni-freiburg.de
Tel.: +49-761-2032862, Fax: +49-761-2032860

Here we report for the first time reliable recording of multiple single-unit spike activity with MEAs in acute slice preparations of the cerebellum and discuss the recording conditions in view of the equivalent circuit commonly used. We conclude that extracellular recording of spike potentials with MEAs is not prevented by the layer of debris. In slice preparations of the cerebellar cortex and the neocortex, single- and multiunit spike signals and LFPs were reliably recorded, allowing visualization and analysis of the network activity on different time scales.

Materials and methods

Spike activity was recorded with substrate integrated thin-film MEAs (Multi Channel Systems, Reutlingen, Germany) as described previously (Egert et al. 1998; Hämmerle et al. 1994; Janders et al. 1996; Nisch et al. 1994). Briefly, MEAs consisted of 60 electrodes etched from gold layers on a 5×5-cm glass carrier using thin-film photolithography. Each MEA electrode was a disk of 10 or 20 µm diameter at the tip of a conducting gold lead, insulated with silicon nitride (Si_3N_4). The electrode surface was coated with a layer of titanium nitride (TiN), increasing the effective surface area of the electrodes and thus lowering electrode impedance. Electrodes were arranged in an 8×8 pattern on a 100- or 200-µm grid. A glass ring (diameter 20 mm; glued to the base plate with silicone rubber; Sylgard 184, World Precision Instruments, Berlin, Germany) formed a recording chamber with a volume of 1.5 ml).

The signals from the MEA electrodes were amplified (×1200), band-pass filtered (10–3200 Hz) with a 60-channel amplifier, and sampled at 25 kHz/channel on 60 channels simultaneously (MEA-60 System, Multi Channel Systems, Reutlingen, Germany). Data were analyzed offline using a specifically designed Matlab Toolbox[1] (Mathworks, Natick, MA). In some experiments we tested for cross talk between neighboring MEA electrodes and compared MEA to conventional tungsten electrodes (TEs). The voltage at two neighboring MEA electrodes and an additional TE (12 MΩ, WPI) was sampled at 20 kHz with a CED 1401/Spike 2 (Cambridge Electronic Design, Cambridge, UK). The signal from the external TE was amplified using either 1 of the 60 MEA amplifier channels or a conventional differential amplifier (A-M Systems, Everett, WA; ×1000, 0.3–5 kHz).

MEAs were used repeatedly and were cleaned before each experiment with a neutral laboratory detergent in an ultrasonic bath (2% Ultrasonol 7, Carl Roth, Karlsruhe, Germany, 10 min) and subsequently rinsed in distilled water.

Coating

To improve tissue adhesion, MEAs were coated with cellulose nitrate (CN, Schleicher & Schuell, Dassel, Germany) dissolved in methanol (0.14 mg/ml). About 4 µl of this solution was spread out over approximately 25 mm^2 around the central recording area and dried in air.

Preparation of slices

Parasagittal and horizontal cerebellar slices (300 µm thick) were prepared from Sprague-Dawley rats on postnatal days 9–28 as described previously (Heck 1993). Animals were anesthetized with diethylether. The brain was quickly excised and rinsed in ice-cold (<4°C) artificial cerebrospinal fluid (ACSF; contents in mM: NaCl 132.0, KCl 2.0, KH_2PO_4 1.2, $MgSO_4$ 1.1, $NaHCO_3$ 19.0, $CaCl_2$ 2.5, D-glucose 10.0, continuously gassed with 95% O_2, 5% CO_2). Slices were cut with a vibratome (Microslicer DTK-1000, DSK, Japan) and stored at room temperature. Recordings were performed at room temperature (24°C). In some control experiments, Ca^{2+} in the ACSF solution was replaced with Mg^{2+}, or tetrodotoxin (2 µM, Sigma-Aldrich, Deisenhofen, Germany) was added to the bath solution. Slices were perfused for several minutes before examination of the effects.

[1] [http://www.brainworks.uni-freiburg.de/projects/mea/meatools/overview.htm]

Electrode resistance

The ohmic component of the electrode impedance was assessed for MEA electrodes alone and for MEAs with a slice mounted on the electrode surface using the impedance measuring facility of an extracellular amplifier (A-M Systems, Everett, WA; delivering 1 µA current at 1 kHz with capacitance compensation). The reproducibility of this measurement was ±50 kΩ (resistance range 0.3–2 MΩ) with capacitance compensation and readout on an oscilloscope screen.

Spatial integration/resolution of electrodes

To evaluate the spatial resolution of MEA electrodes and possible overlap of neuronal populations recorded with neighboring electrodes, we calculated cross-correlograms of spike trains and spike-triggered averages of raw waveforms recorded on several pairs of MEA electrodes. Spikes were detected offline using a threshold criterion and sorted according to their principal component composition. Any spike that could not be assigned clearly to one neuron was discarded from the analysis.

In a typical experiment, an MEA electrode picking up single-unit spike activity with good signal-to-noise ratio (SNR) was chosen as the reference electrode (RE). After spike detection and sorting (see below) cross-correlations were calculated for spike trains recorded at RE and those on directly neighboring electrodes that picked up spikes at an SNR sufficient for spike sorting. For all eight neighboring electrodes, a signal average was calculated triggered on the single-unit spikes recorded at RE. This spike-triggered average was used to estimate the electrical field produced by the trigger unit recorded at RE.

As a measure of the noise bandwidth, we calculated the standard deviation of short periods (several milliseconds) of recordings without detectable spikes. In a gaussian distribution, more than 99% of the sampled values lie within a range of ±3 times the standard deviation (σ) around the mean. We thus set $\pm 3\times\sigma$ of the background noise (calculated from segments without spike activity) as the minimum reasonable threshold value (θ) for spike detection in a noisy signal. For the assessment of duplicate spike detection on neighboring MEA electrodes, signals that did not cross θ were defined as undetectable.

Spatial extent of the spike signal

To identify the location of a selected cell recorded at an MEA electrode, again termed RE, and the size of its detectable electrical field, we probed the surrounding tissue volume with an external electrode. Extracellular glass micropipettes (3–6 MΩ, 0.1–3 kHz, WPI DAM80 amplifier) were used in this case since the vertical position of the tip could be determined. For this purpose, a light guide was attached to the end of the electrode to illuminate its tip. At each position, the signals at RE and micropipette were recorded simultaneously for 2 min. To prevent damage to the cell under observation, we recorded at positions in a plane approx. 40 µm above the MEA surface. The spikes detected at RE were sorted as described above to isolate a single-unit signal. For our purposes it was important to ensure that these spikes stemmed from a single unit. We therefore accepted an underestimation of the spike rate by the sorting procedure to minimized ambiguities. To ensure stable spike detection during the experiment we chose trigger spikes from a population of large spikes. Under these conditions, the shape of the spikes recorded at both electrodes was comparable as long as spikes were found at all at the micropipette. Comparing corresponding minima and maxima of the spike peaks thus gave a robust indication of the decay of the electric field with distance from the source.

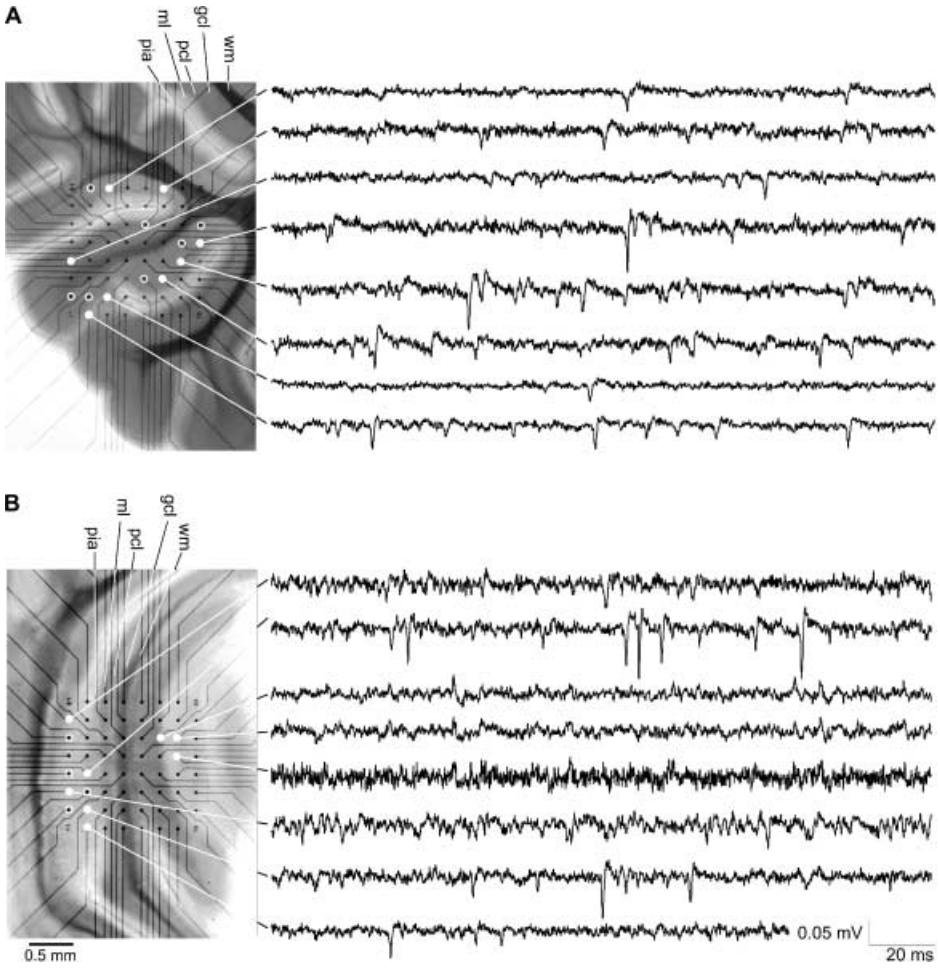

Fig. 1 Examples of continuous MEA recordings. Sample recordings from a parasagittal **(A)** and a horizontal cerebellar slice **(B)** from a P15 and a P14 rat, respectively. *The micrographs* show the cerebellar slices mounted on the MEA electrodes. *The traces* are typical recordings in these particular preparations from electrodes marked with *filled circles* (activity was also found on electrodes marked by *open circles*) (*wm* white matter, *gcl* granule cell layer, *pcl* Purkinje cell layer, *ml* molecular layer, *pia* pial surface)

The identified spikes (reference spikes) were then used as a trigger for spike-triggered averaging (STA) of the signal recorded from the micropipette. This average thus gives the waveform found at the micropipette when a reference spike was detected. We then determined minima and maxima of the STA $(\bar{X}_{xy})$ at times corresponding to the minimum and maximum of the average reference spike respectively $(\bar{X}_{ref_{xy}})$ for each recording position with the coordinates *x*, *y* at a given height above the MEA electrodes. To compensate for variations of the absolute size of the spikes during the experiment, we describe the extracellular field as the ratio of these values found at the micropipette position and the corresponding value of the simultaneously recorded reference spikes (e.g., $\min(\bar{X}_{xy})/\min(\bar{X}_{ref_{xy}})$, $\max(\bar{X}_{xy})/\max(\bar{X}_{ref_{xy}})$. This results in one ratio for minima, maxima, and total amplitude, respectively, at each recording site. The value thus obtained is a relative measure of the magnitude of the signal at the micropipette positions. From these, we estimated the continuous field structure by bicubic interpolation of the corresponding ratios for a plane supported at the recording positions.

Results

Recordings in sagittal cerebellar slices

Cerebellar Purkinje cells (PCs) have a flat, fan-shaped dendritic tree oriented parallel to the sagittal plane. Owing to their shape, PCs in sagittal slices remain largely undamaged, except for those immediately at the surface. Furthermore, because soma and dendrite lie in the same sagittal plane, intact Purkinje cell somata can be found in high density close to the surface of the slice. In slices mounted onto MEAs, the recording electrodes cover an area of one to two lobuli, depending on the animal's age. Molecular, Purkinje cell, and granule cell layers, and white matter are readily distinguished. Purkinje cell somata form a thin (30–50 µm) layer with about 400 cells/mm^2. The molecular layer extends between the Purkinje cell layer (PCL) and the pial surface. It contains the PC and Golgi cell dendrites, parallel fibers, and the somata and dendrites of the inhibitory basket and stellate cells. The granule cell layer between PCL and white matter holds the granule cells, the ascending part of their axons and Golgi cell somata and axons. Examples for signals recorded in these layers in sagittal and horizontal slices are shown in Fig. 1. The distribution of electrodes beneath the layers of the cerebellar slices is given in Table 1.

Single-unit spikes were reliably recorded with MEAs from acute sagittal slices of the cerebellum (Fig. 1A), with SNR ratios up to 10. Electrodes detected mostly multiple single-unit activity in all tissue layers. The overall fraction of electrodes detecting spikes in sagittal slices was 29.5% (*N*=20 slices), with the probability of spike detection varying between different layers of the cerebellar cortex. Electrodes located underneath the PCL

Table 1 Distribution of the electrode positions over cortical layers. Fraction of electrode positions with successful detection of spike activity in sagittal slices. Signal quality was rated on a scale of 0–5 during recording, with 0 indicating no spikes and 5 an SNR of at least 3×θ. Because of its extent, most electrodes are located in the granule cell layer. The relative yield of spikes bearing electrodes and signal quality was, however, best in the Purkinje cell layer, i.e., closest to the Purkinje cell somata. *Numbers in parentheses* give the standard deviation (*ML* molecular layer, *PCL* Purkinje cell layer, *GCL* granule cell layer, *WM* white matter)

	ML	PCL	GCL	WM	N_{slices}
Electrode distribution	29% (7)	14% (6)	36% (7)	20% (8)	15
Spike bearing electrodes	29% (26)	39% (31)	38% (22)	20% (15)	17
Subjective signal-to-noise ratio	2.4 (0.94)	3.3 (1.43)	2.7 (0.88)	1.7 (0.94)	17

had the highest probability of spike detection. Spike polarity reflected the position of the electrode relative to the signal source, i.e., negative close to the soma or positive in the dendritic tree. Spikes found in the Purkinje or granule cell layers were negative, matching the cerebellar architecture, and positive peaks were regularly detected in the molecular layer. The temporal structure of the spike trains and the spike rates were comparable to those found with conventional microelectrode recordings.

Comparison of MEA and conventional tungsten electrodes

Spikes were also detected in slices cut horizontally, with an SNR comparable to what we found in sagittal slices (Fig. 1B), although in horizontal slices there were generally fewer recording sites with spike activity. Recording of single-unit spike activity was most successful in slices from animals younger than 21 days postnatal. The probability of detecting spike activity, but not their SNR, decreased thereafter. We could not record spike activity in slices from animals older than 28 days postnatally. Both sagittal and horizontal slice preparations were viable for up to 16 h. Spike activity was abolished by tetrodotoxin (TTX), withdrawal of Ca^{2+} or cooling of the slice to 11°C.

To compare recording properties of MEA and conventional electrodes, we simultaneously recorded with two neighboring MEA electrodes that both showed single-unit spike activity and with one external tungsten microelectrode or glass micropipette. The TE was positioned close to one of the MEA electrodes such that both would pick up the same unit spike (Fig. 2A). To compare spike shapes and to test for duplicate detection of a given unit, we calculated spike-triggered averages of the signal at three neighboring electrodes. Defining in turn the spikes of each of the three electrodes as trigger events, we generated spike-triggered averages of the signals on the other two electrodes. Spike shapes recorded with MEA and TEs were comparable. The unit spike recorded on electrode MEA 1 left no visible trace in the spike-triggered averages generated from the signals on MEA 2 and the TE (Fig. 2B, upper row). The electrode MEA 2 and the TE picked up spikes from the same unit. Thus, the average of the TE signal triggered on the spikes recorded on MEA 2 looks like the averaged TE signal,

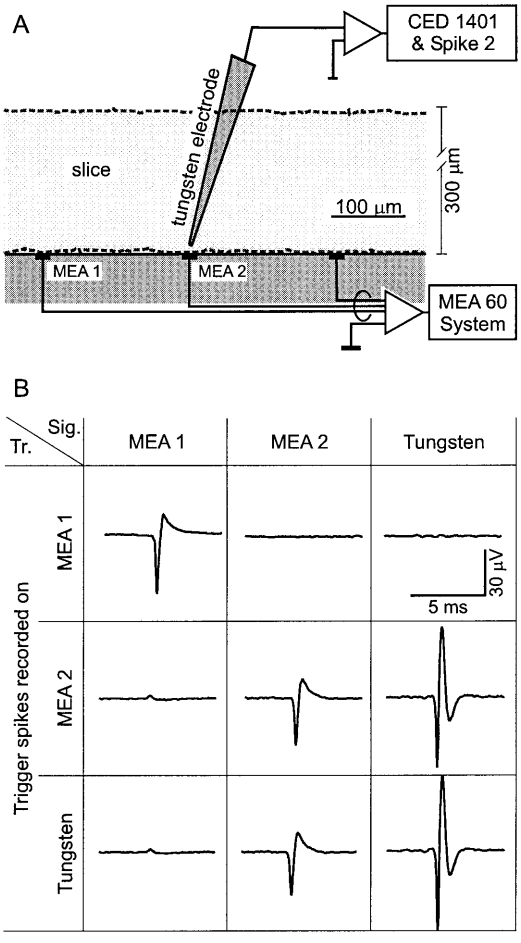

Fig. 2A, B Comparison of spike detection characteristics of MEA and conventional tungsten microelectrodes. **A** Schematic diagram of the recording situation. Electrode distances are drawn to scale. Two neighboring MEA electrodes (*MEA 1, MEA 2*), both of which picked up spike activity, were selected and a TE tip was positioned about 10 µm above MEA electrode 2. **B** Each plot in the matrix shows a spike-triggered average of the data recorded on one electrode (indicated in the column title), triggered on 300–500 spikes of a unit recorded on the electrode indicated by the row title. Each of the three plots on the top left to bottom right diagonal thus shows the average unit spike signal on the respective electrode. The spike shapes on MEA and TEs differ because of the different filter properties of the respective amplifiers

triggered on its own spikes (Fig. 2B, middle and lower row, middle and right column). The average signal recorded on the neighboring MEA 1 electrode triggered on the MEA 2 or TE spike (Fig. 2B, left column, middle

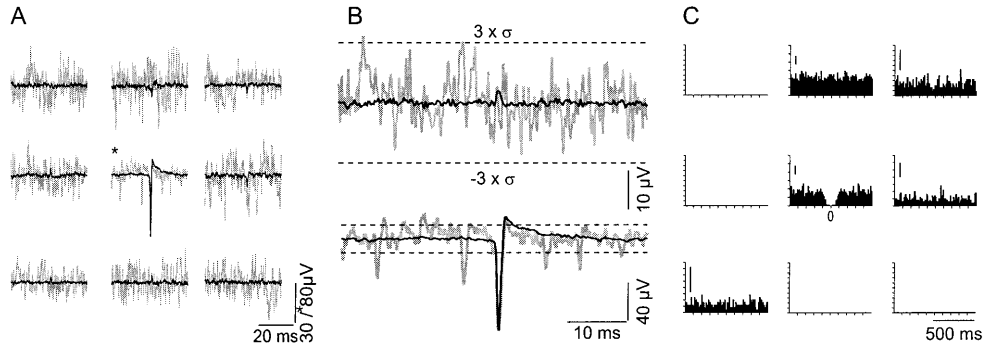

Fig. 3A–C Relevance of the signal overlap observed. **A** Spike-triggered averages (*black*) in comparison to typical single-trial traces (*gray*) on RE (*central plot*) and on the eight immediately neighboring MEA electrodes. The peaks detected by spike-triggered averaging are far smaller than the background noise level. **B** The peaks revealed by spike-triggered averaging are well below the useful limit for spike detection (±3×σ), i.e., spikes detected on neighboring electrodes appear, if at all, only as a sub-threshold signal. **C** If background noise were additive, small spikes could occasionally cross the threshold and contribute to an apparent correlation of spike trains at neighboring electrodes. In this example, we calculated the cross correlations between the spike trains at the outer MEA electrodes with that of the center electrode (the autocorrelation is given for this electrode, with the center peak graphically removed for clarity). These cross correlations did not reveal significant peaks, indicating that each electrode gives an independent sample of the local spiking activity. *Empty axes* indicate electrode positions without detectable spike activity. *Vertical bars in* **C** indicate 10 counts/bin (bin width 10 ms)

and lower row) shows a positive peak. This peak was smaller than the noise band defined by the θ criterion and, thus, below the threshold for spike detection (see below).

To assess the possibility of duplicate detection of a neuron at neighboring MEA electrodes, we calculated cross-correlograms of the spike trains and spike-triggered averages of the signal traces.

Large reference spikes, presumably generated by cells close to RE, produced only minute voltage peaks at surrounding electrode positions (Fig. 3A, 200 and 283 µm between neighboring electrodes on either side and along the diagonals, respectively). These averaged voltage peaks were well within the noise band defined by θ (Fig. 3B). We obtained the same results with external TEs placed at comparable distances to an MEA electrode which recorded the trigger spikes (Fig. 2B). When small spikes, presumably originating from neurons at some distance from RE and located between two electrodes, were used as reference spikes, the spike-triggered average sometimes showed peaks larger than θ on one of the neighboring electrodes. Occasionally, electrodes in the molecular layer detected a positive going peak, synchronous to spikes at a corresponding location in the PC layer, suggesting dendritic sources (e.g., Fig. 1B, 3rd and 4th traces). We did not find any clear triphasic spikes that would typically be expected for axonal sources.

Theoretically, even small spikes added to the background noise in a systematic, e.g., temporally correlated way, may influence spike detection when low voltage thresholds are used. We further tested for correlations between spike trains from neighboring electrodes in sagittal slices. Spikes in these trains were again detected when crossing θ. Such spike trains did not show significant correlations, independent of spike size (40 pairs from spike populations on pairs of neighboring electrodes, see Fig. 3C). This is in agreement with the expectation, based on the neuronal connectivity in sagittal cerebellar slices, where the only excitatory fibers run perpendicular to the slice plane. The only anatomically possible interaction between PC would be inhibitory through synaptic input from basket, stellate or other PCs. However, cross-correlograms did not show negative correlations either.

Estimation of the electrical field of the neuron detected

By scanning the slice in the vicinity of one RE with a micropipette, we estimated the approximate extent of the reference unit's detectable electrical field. Measurements were made at various locations in a plane parallel to the MEA surface (white circles in Fig. 4B). For each location, the amplitude ratios of the spike-triggered averages (local/reference signal) were calculated. From these values, the amplitude ratios for intermediate positions were estimated by bicubic interpolation. From the resulting matrix, a surface plot was generated. The maximum in this plane of ratios indicates the likely position of the reference unit's soma, i.e., the signal source. This was typically found within a radius of approx. 30 µm around the MEA electrode center.

The value of the R_s, which, according to the equivalent circuit, is the parameter most critical for the SNR of spike recordings, cannot be measured directly. For an approximation of R_s, we calculated the difference between the ohmic component of the MEA electrode impedance at 1 kHz with and without the slice tissue in place. Surprisingly, there was no detectable difference of the electrode impedance between these conditions. Likewise, with the slice mounted on the MEA surface, there was no detectable difference in impedance between electrodes picking up spike signals with good SNR and electrodes that did not pick up any spikes.

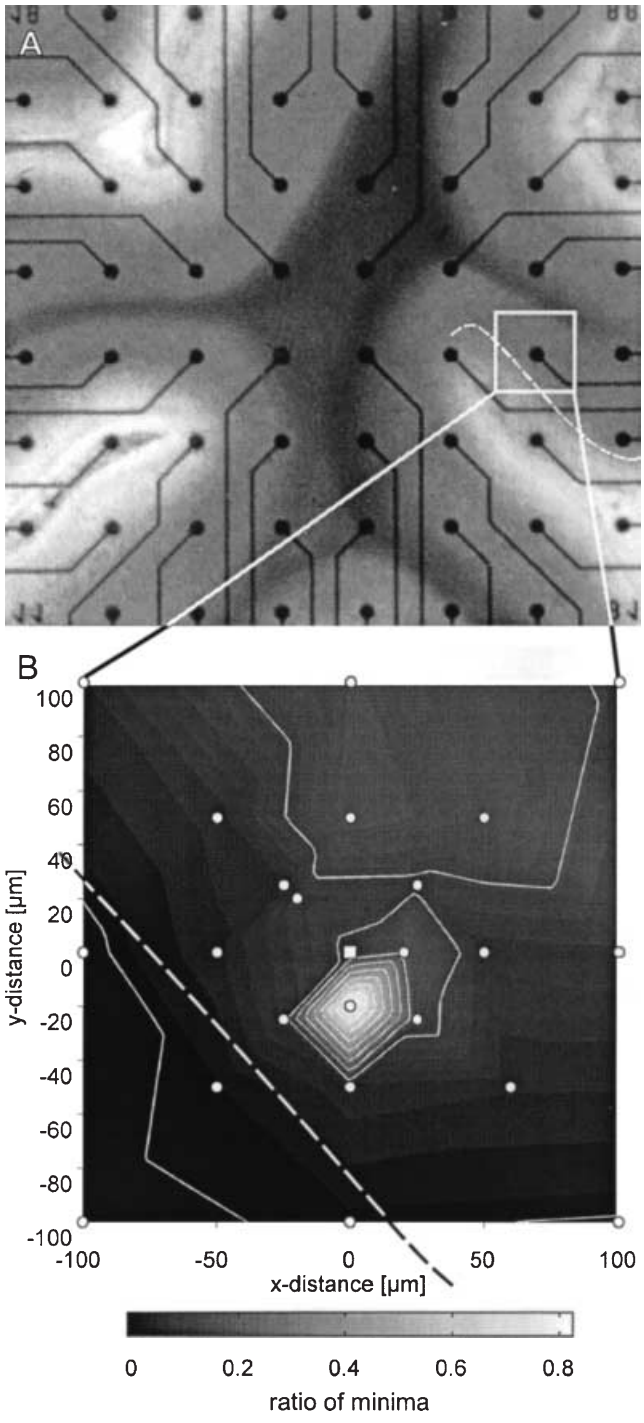

Fig. 4A, B Estimate of the electrical field around a reference unit. **A** Parasagittal slice of the cerebellum with the recording area (*square*) and the position of the Purkinje cell layer marked. **B** An external glass micropipette was used to determine the average electrical signal generated by the reference unit at the positions marked with *white circles*. These support locations (40 µm above the MEA surface) were used for bicubic interpolation of the relative field strength (relative amplitudes with respect to the reference electrode) and the location of the reference unit in the plane of the slice. The maximum spike size (*bright area*) on the micropipette was found 20 µm from the MEA electrode (*small square*), which is outside the geometrical electrode radius (10 µm). The example suggests that it is not necessary to establish membrane contact with the cell body for spike recording. The shape of the spikes found at that site and the position of the MEA electrode indicate that a cell body in the Purkinje cell layer (*dashed line in* **A**) was recorded (contour lines mark steps of 0.1)

Discussion

We have shown here for the first time that recording of single-unit spike activity in acute slice preparations using planar, substrate-integrated microelectrode arrays is possible. The comparison of MEA with conventional TEs showed that both types of electrodes had very similar electrical properties in terms of spike shapes and spatial resolution. This suggests that recording from the underside of the slice has no disadvantages in this experimental configuration, even though the supply of vital substances and oxygen by diffusion might be more difficult on this side than on the exposed upper surface of the slice, where single electrode recordings are usually performed. Although spike-triggered averages in some cases revealed small peaks, these were well within the background noise band and did not contribute to spike detection. Since SNRs at soma-proximal positions were much higher than SNRs at any other position and dropped rapidly with distance, our recordings reflect local spike activity almost exclusively. This is illustrated by the structure of the electrical field of the reference units. The observation that spike trains with spikes of any size recorded from neighboring electrodes were uncorrelated suggests that even cells located between electrodes may not be detectable on both. It must be kept in mind, however, that spike sorting may not isolate single-unit spikes from multi-unit populations of small spikes, which could obscure correlations of the resulting time series (Gerstein 2000; Bar-Gad et al. 2001).

Equivalent circuits developed to describe the conditions for recording spike activity with surface integrated electrodes demand that the resistance between recording site and reference electrode R_s be much higher than that between recording site and signal source (Fromherz et al. 1993; Grattarola and Martinoia 1993). The lowest value used for R_s in a modeling study was 1 MΩ (Grattarola and Martinoia 1993). According to Fromherz et al., high R_s values require intimate contact between the membrane of the recorded neuron and the electrode (Fromherz et al. 1991). Furthermore, theoretical considerations about the recording situation with extracellular electrodes suggested that the SNR depends on the value of the R_s between the signal source and the ground electrode (Fromherz and Stett 1995; Grattarola and Martinoia 1993). Our results indicate that assumptions made about the electrical equivalent circuit, especially about a high value for R_s as a prerequisite of single-unit spike recording, are incorrect. The resistance of the MEA electrodes was not changed when a slice was mounted, and resistances of electrodes that picked up spike activity and those that did not were identical within the resolution of our measurement (±50 kΩ).

While these values may not be a precise measure of the absolute value of the impedance, the lack of a significant change of the electrode impedance indicates that R_s is likely not in the MΩ range as was expected. They further suggest that the distance over which an electrode picks up signals from a spiking neuron is larger than might be expected from previous model considerations

(Fromherz et al. 1991, 1993; Grattarola and Martinoia 1993).

We propose that the most important difference between cerebellar and other slice preparations is the presence of ongoing spontaneous spike activity at a high rate in cerebellar slices. Because of the fan-shaped anatomy of the Purkinje, stellate, and basket cell dendrites spreading in the sagittal plane, a sagittal cut presumably damages these dendrites only slightly. Therefore, sagittal cerebellar slices most likely have only a thin layer of dead or injured cells. They may be special in that healthy, active neurons may be closer to the MEA electrodes than in tissues in which neurons branch more homogeneously in all three dimensions and, hence, may suffer more damage by the slicing procedure. However, we also obtained reliable single-unit spike recording, from horizontal slices, whose surface is perpendicular to the plane of the PC dendritic tree, in neocortical slices and, as a component of field potential recordings, in acute hippocampus slices (data not shown). We assume that there is a layer of dead and injured cells on horizontal slices similar in thickness to the debris layer on hippocampal and neocortical slices. It is interesting to note that in standard slice preparations (without MEAs) inspected with infrared video microscopy healthy cells are found 15–30 µm from the slice surface (data not shown), which is in good agreement with the dimensions of the electrical field found in our experiments. From these results we conclude that recording of single-unit spike activity in acute slice preparations with MEA technology does not critically depend on the thickness of the debris layer (and, thereby, on R_s).

The recording of single-unit spike activity from many locations simultaneously in acute preparations extends the applicability of the MEA technology to the investigation of fast dynamics of neural network activity. This is a particularly interesting aspect in view of the increasing evidence for the importance of dynamic interactions between groups of neurons on a millisecond time scale (Abeles et al. 1993a, 1993b; Ahissar et al. 1992; Riehle et al. 1997; Diesmann et al. 1999). MEA technology thus provides a new important and easy to use in-vitro tool for the investigation of spiking neural networks.

Acknowledgements We thank the NMI Reutlingen for providing a recording setup and MEAs for some of the experiments. We thank Stefanie Maier for excellent technical assistance, Armin Brandt for the micrograph and dataset used in Fig. 1B, and Markus Diesmann and Thomas Wachtler for helpful comments on the manuscript. Parts of this work were supported by grant no. 0310965 from the German BMBF.

References

Abeles M, Bergman H, Margalit E, Vaadia E (1993a) Spatiotemporal firing patterns in the frontal cortex of behaving monkeys. J Neurophysiol 70:1629–1638

Abeles M, Prut Y, Bergman H, Vaadia E, Aertsen A (1993b) Integration, synchronicity and periodicity. In: Aertsen A (ed) Brain theory. Elsevier, Amsterdam, pp 149–181

Ahissar E, Vaadia E, Ahissar M, Bergman H, Arieli A, Abeles M (1992) Dependence of cortical plasticity on correlated activity of single neurons and on behavioral context. Science 257: 1412–1415

Bar-Gad I, Ritov Y, Vaadia E, Bergman H (2001) Failure in identification of overlapping spikes from multiple neuron activity causes artificial correlations. J Neurosci Methods 107:1–13

Brivanlou IH, Warland DK, Meister M (1998) Mechanisms of concerted firing among retinal ganglion cells. Neuron 20:527–539

Connolly P, Clark P, Curtis ASG, Dow JAT, Wilkinson KCDW (1990) An extracellular microelectrode array for monitoring electrogenic cells in culture. Biosens Bioelectron 5:223–234

Diesmann M, Gewaltig MO, Aertsen A (1999) Stable propagation of synchronous spiking in cortical neural networks. Nature 402:529–533

Egert U, Schlosshauer B, Fennrich S, Nisch W, Fejtl M, Knott Th, Müller T, Hämmerle H (1998) A novel organotypic long-term culture of the rat hippocampus on substrate-integrated multielectrode arrays. Brain Res Prot 2:229–242

Fejtl M, Knott Th, Leibrock C, Schlosshauer B, Nisch W, Egert U, Müller T, Hämmerle H (1998) Multi-site recording as a new tool to study epileptogenesis in organotypic hippocampal slices. Eur J Neurosci 10(Suppl 10) 44

Fromherz P, Stett A (1995) Silicon-neuron junction: capacitive stimulation of an individual neuron on a silicon chip. Phys Rev Lett 75:1670–1673

Fromherz P, Offenhäusser A, Vetter T, Weis J (1991) A neuron-silicon junction: a Retzius cell of the leech on an insulated-gate field-effect transistor. Science 252:1290

Fromherz P, Müller CO, Weis R (1993) Neuron transistor: electrical transfer function measured by the patch-clamp technique. Phys Rev Lett 71:4079–4082

Gerstein GL (2000) Cross-correlation measures of unresolved multi-neuron recordings. J Neurosci Methods 100:41–51

Grattarola M, Martinoia S (1993) Modeling the neuron-microtransducer junction – from extracellular to patch recording. IEEE Trans Biomed Eng 40:35–41

Gross GW, Rhoades BK, Reust DL, Schwalm FU (1993) Stimulation of monolayer networks in culture through thin-film indium-tin oxide recording electrodes. J Neurosci Methods 50:131–143

Gross GW, Harsch A, Rhoades BK, Göpel W (1997) Odor, drug and toxin analysis with neuronal networks in vitro: extracellular array recording of network responses. Biosens Bioelectron 12:373–393

Hämmerle H, Egert U, Mohr A, Nisch W (1994) Extracellular recording in neuronal networks with substrate integrated microelectrode arrays. Biosens Bioelectron 9:691–696

Heck D (1993) Rat cerebellar cortex in vitro responds specifically to moving stimuli. Neurosci Lett 157:95–98

Janders M, Egert U, Stelzle M, Nisch W (1996) Novel thin film titanium nitride micro-electrodes with excellent charge transfer capability for cell stimulation and sensing applications. 48–48. 1996. Bridging Disciplines for Biomedicine, Proceedings of the 18th Annual Conference of the IEEE Engineering in Medicine and Biology Society

Kamioka H, Maeda E, Jimbo Y, Robinson HPC, Kawana A (1996) Spontaneous periodic synchronized bursting during formation of patterns of connections in cortical cultures. Neurosci Lett 206:109–112

Meister M, Pine J, Baylor DA (1994) Multi-neuronal signals from the retina – acquisition and analysis. J Neurosci Methods 51:95–106

Nisch W, Böck J, Egert U, Hämmerle H, Mohr A (1994) A thin film microelectrode array for monitoring extracellular neuronal activity in vitro. Biosens Bioelectron 9:737–741

Riehle A, Grün S, Diesmann M, Aertsen A (1997) Spike synchronization and rate modulation differentially involved in motor cortical function. Science 278:1950–1953

Wheeler BC, Novak JL (1986) Current source density estimation using microelectrode array data from the hippocampal slice preparation. IEEE Trans Biomed Eng 33:1204–1213

Wheeler BC, Eden JG, Brewer GJ (1989) Patterned growth of hippocampal neurons on microcircuits. Soc Neurosci Abstr 15:1036–1036